

WEATHER RADAR VERSUS 2D-VIDEO-DISTROMETER DATA

M. Schönhuber¹⁾, H.E. Urban¹⁾, J.P.V. Poiarés Baptista²⁾, W.L. Randeu³⁾ and W. Riedler³⁾

1) Institute for Applied Systems Technology, JOANNEUM RESEARCH, Graz/Austria

2) ESA/ESTEC (XEP), Noordwijk, The Netherlands

3) Institute of Communications and Wave Propagation, Technical University Graz/Austria

ABSTRACT

The size, shape, velocity and orientation of precipitation particles are of fundamental importance in the field of telecommunications, especially in the interpretation of weather radar data. The 2D-Video-Distrometer presents measurements classifying precipitation as well as full particulars on single hydrometeors. Data have been recorded since early 1992, a tropical rain measurement campaign has been performed as well. Examples showing rain events, snowfall and melting particles are given. Comparisons with precipitation characteristics described in literature are presented, particularly the measured size distribution, the vertical fall velocity and the shapes of rain drops are investigated. In many cases these comparisons reveal a good match, however there are a number of examples exhibiting differences between observations and standard models. Especially in thunderstorm situations drop distortions due to horizontal wind forces and significant deviations from expected fall velocities are to be mentioned. In addition to these basics, simultaneous measurements by the 2D-Video-Distrometer, by a standard tipping bucket rain gauge and by the dually polarized, frequency agile weather radar Hilmwarte (Graz/Austria) have been carried out. Radar data are interpreted in terms of precipitation parameters as well as distrometer data in terms of radar reflectivities. Time series plots are given, results are discussed.

1. INTRODUCTION

Generally in the fields of remote sensing and telecommunications, specifically in the area of weather radar, knowledge on details of hydrometeors is of great importance. Various types of distrometers measure some of the interesting parameters and in many cases some others have to be set to predefined values taken from the literature. The 2D-Video-Distrometer measures full particulars of single hydrometeors and thereby quantity and rate of precipitation. These data allow validations of literature models for the parameters of single hydrometeors like shape and velocity of raindrops and validations of weather radar data interpretation.

2. SINGLE PARTICLES' CHARACTERISTICS

2.1 Raindrops

The nature of raindrops has been studied in detail by many researchers. Well known publications present clear models on the shape of raindrops. These models either suggest that raindrops are similar to oblate spheroids and that they are defined by their axial ratio or they define a function describing the surface of a body of revolution in polar coordinates. Photographs have been taken as well. However, the discussion on the nature of raindrops cannot be considered to be finished. Quite on the contrary there are some more questions on drop characteristics which are far away from being well answered. Aspects like drop oscillation and drop orientation angle are often discussed. The results of the 2D-Video-Distrometer allow new answers to these questions, as it records the front- and the side view of each drop reaching the measuring area. The resolution of the digitizing grid is in the order of 0.25 mm, thus presenting detailed views of drops. The measured shapes of the drops have to be classified somehow. In events of homogenous stratiform rain, this could be done according to models available in the literature, as drop shapes follow these models rather well. In storm events raindrops present various irregular shapes. In spite of all irregularity of shapes, the ratio of the drop's maximum vertical to its maximum horizontal dimension referred to the ground is always available and easily determined. In the course of this paper that ratio shall be called "oblateness", although there is some inaccuracy as that ratio generally is not identical with the oblateness of spheroids. Only with drops precisely following the spheroidal model at zero orientation angle the oblateness defined by the ratio maximum height to maximum width is identical to the spheroidal oblateness.

Figure 1 presents first of all the calibration status of the 2D-Video-Distrometer. 827 high precision spheres with integer values of diameter have been dispensed into the measuring area. The oblateness of these spheres is identical to 1. The crosses mark the desired measurement results, the dots indicate the actual ones. Due to digitizing effects there is some spread around the ideal positions. Figure 2 gives for the 4 mm diameter spheres the distribution of oblateness. This figure pres-

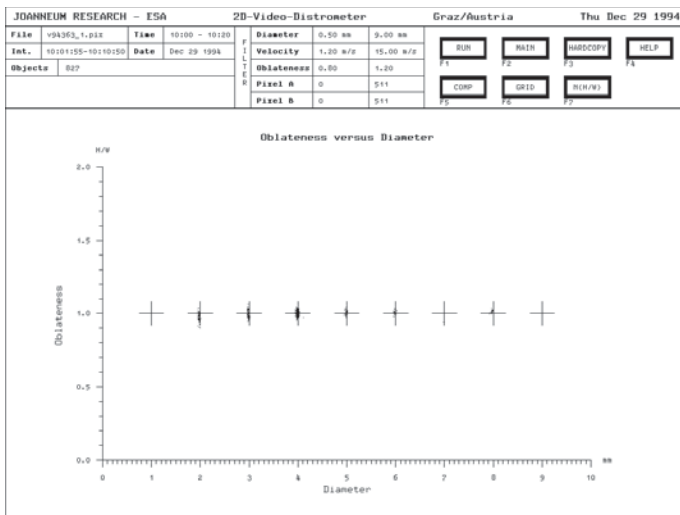


Figure 1: Calibration status of 2D-Video-Distrometer (oblateness of spheres vs. diameter)

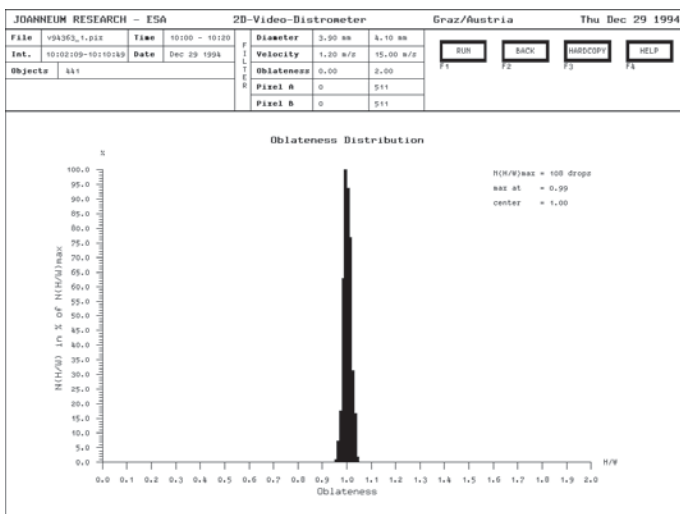


Figure 2: Distribution of oblateness of calibration spheres

resents a clear system analysis for the purpose of shape measurements. What does the oblateness distribution look like in rain? Figure 3 presents the distribution of oblateness of 29 drops with 4 mm diameter (3.9 - 4.1 mm) in a thunderstorm situation. The oblateness is widely spread around its mean value 0.97. That mean is far away of what one would expect from the literature e.g. 0.782 after Pruppacher and Beard (1970). Comparisons to other events have shown, that in storm situations similar data have been recorded, events with homogenous rain without wind are different. Figure 4 again presents drops of 4 mm equivalent sphere diameter. These data have been recorded during an experiment with artificial rain. On a calm day drops have been dispensed with a fall distance of more than 35 meters. As the distrometer was installed directly beneath the dispensing equipment the influence of even light wind was omitted, as drops effected by wind did not reach the 10 cm * 10 cm catchment area of the distrometer. 151 drops with equivalent diameters between 3.9 and 4.1 mm have been counted. The mean value of their oblatenesses is 0.8, well matching with

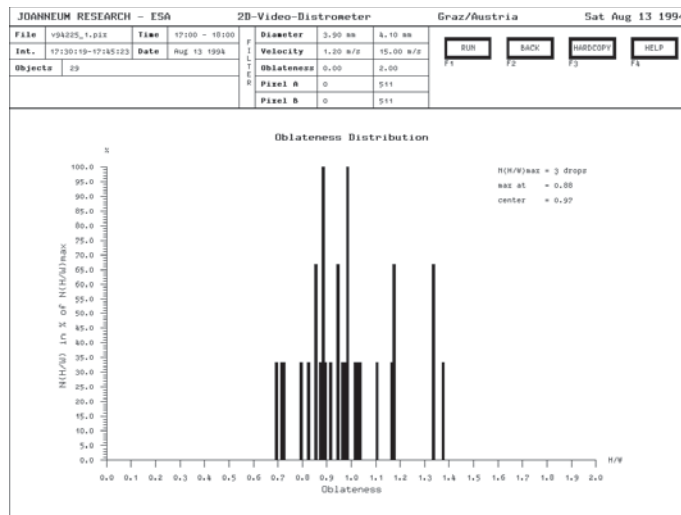


Figure 3: Oblateness distribution in storm

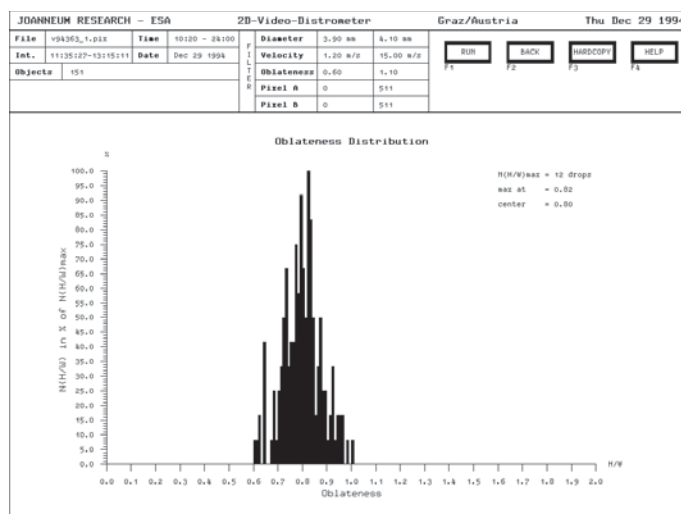


Figure 4: Oblateness distribution in situation without wind

literature values, precisely meeting the values of Morrison and Cross (1974). Certainly the spread around the mean is much bigger than in figure 2, presenting the calibration spheres. That spread cannot only be due to the fact that figure 4 engages drops from 3.9 to 4.1 mm whereas figure 2 is based on precise 4 mm diameter objects only. Drop oscillation effects are obviously detected here. In storm situations as given in figure 3 not only oscillations cause deviations from the expected oblateness. Three of 29 drops show oblateness values of more than 1.3, indicating "prolate" drops. Figure 5 presents the views of one of these "prolate" drops. That drop is obviously accelerated by the wind and therefore flattened at the side. The drop passes the front view camera (left view in figure 5) from the right to the left side at an angle of around 45 degrees. The side view camera (right view in figure 5) records the drop moving downwards at an angle of around 45 degrees directly into its face. This picture presents quite clearly, that the resulting oblateness of 1.37 is only a numeric value without the meaning of the oblateness of a spheroid. The attempt to derive the

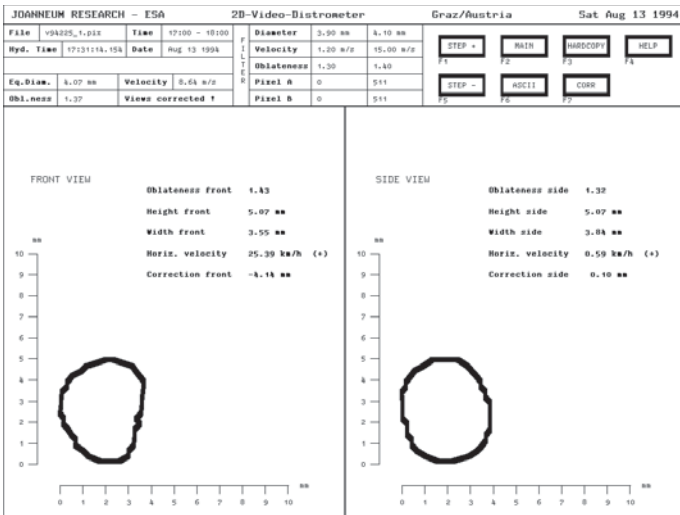


Figure 5: Drop's views in storms

drop's orientation angle from these figures would perhaps lead to some success in the case of the front view picture, where the drop seems to be canted from the vertical nearly to the horizontal direction. A significant difference between storm and homogenous rain situations is further seen in the measurements of fall velocities.

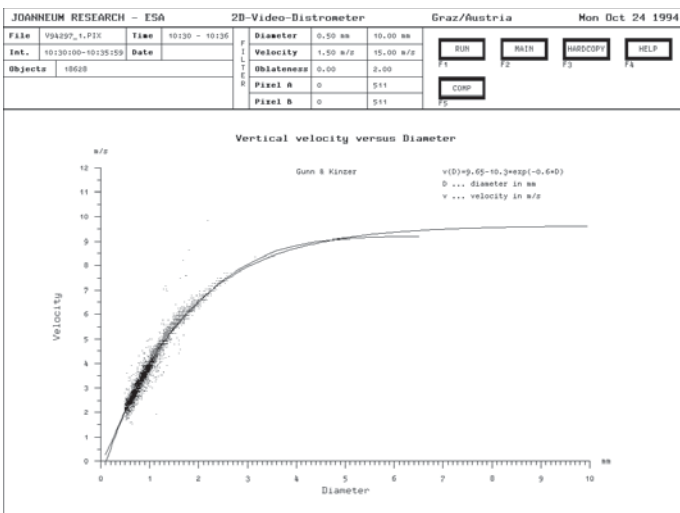


Figure 6: $v(d)$ during widespread rain

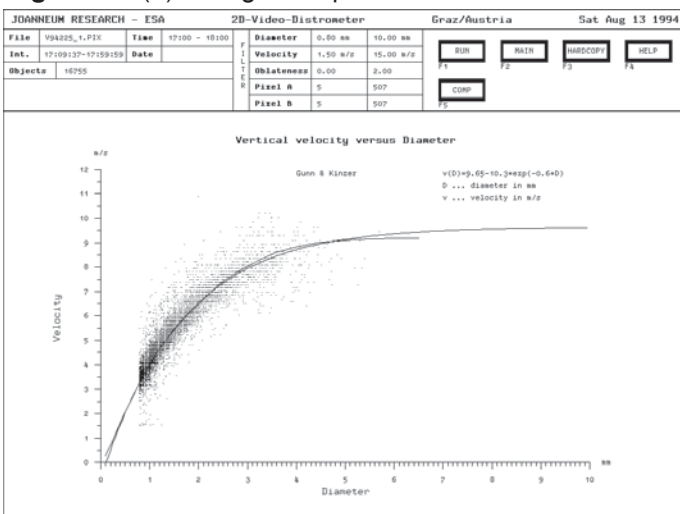


Figure 7: $v(D)$ during storm

Figure 6 presents vertical velocities versus equivolumetric diameter during natural widespread rain, figure 7 shows the same diagram for an even smaller number of

drops than in figure 6, being widely spread around the mean values expected. The solid lines represent values given by Gunn and Kinzer (1949) respectively by Atlas et al. (1973), the dots indicate the measurements. Widespread rain events follow the theory quite well whereas storm events present noticeable deviations.

The results of polarimetric weather radar measurements depend much on drop shapes and orientations. A precise consideration of the measured drop shapes in the radar data conversion algorithms needs detailed calculations of measured precipitation particles' scattering amplitudes, which is beyond the frame of this paper. Measured fall velocities of raindrops allow for a precise normalisation from the number of drops reaching the measuring area to the volume above.

2.2 Melting Particles

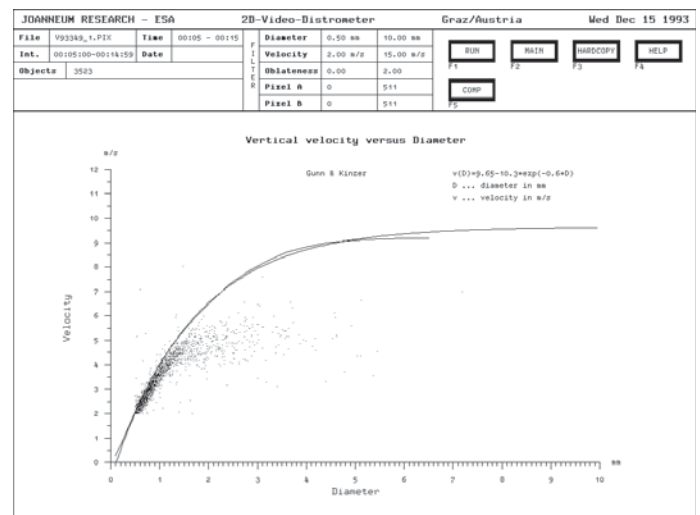


Figure 8: $v(D)$ during melting snow

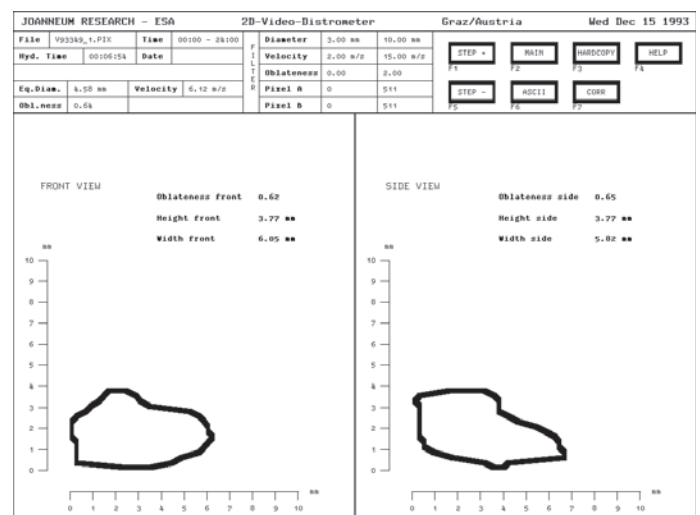


Figure 9: Melting particle: front and side view

Figures 8 and 9 present melting snow. In the vertical velocity versus diameter diagram (fig. 8) it is recognized that small particles are completely melted yet, they follow the theoretical values closely. The bigger particles are still of mixed phase, they have not the terminal fall

velocity of raindrops and they show quite irregular shapes. Figure 9 gives an example.

2.3 Snowflakes

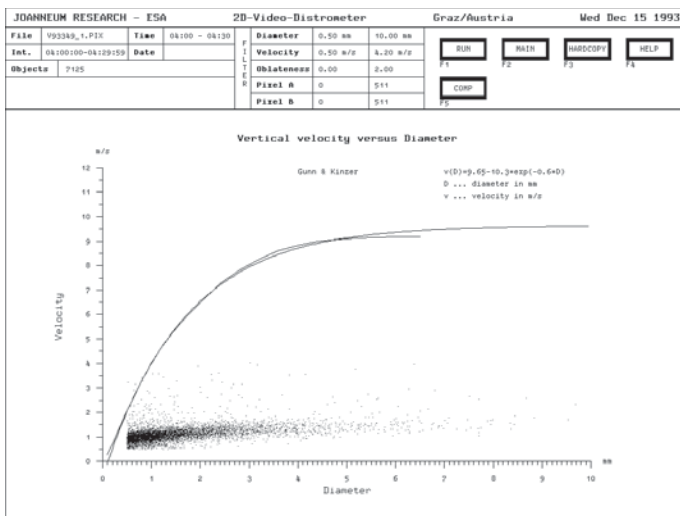


Figure 10: $v(D)$ during snowfall

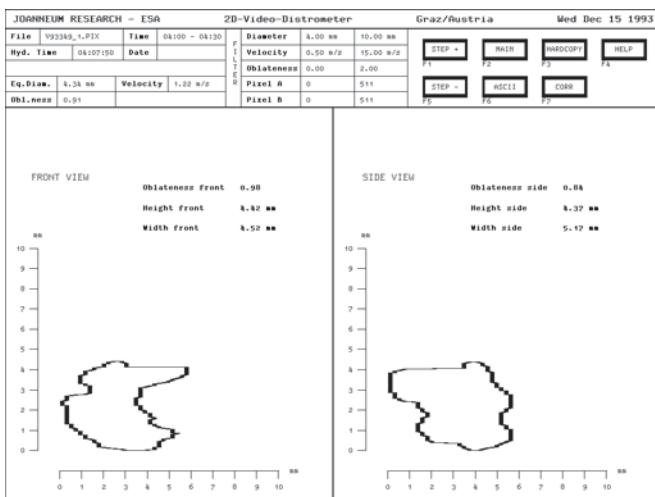


Figure 11: Snowflake: front and side view

Figures 10 and 11 show data acquired during snowfall. The vertical velocity versus diameter diagram (fig. 10) indicates that snowflakes are hardly faster than 2 m/s in fall speed. Snowflakes have all sorts of irregular shadows. It should be noted that only the shadow of snowflakes is recorded, not their detailed threedimensional structure.

3. RAIN INTENSITY MEASUREMENTS

Measurement of rain intensities by remote sensing methods is of great interest in a wide field of applications. The discussion on reliability of such methods needs the verification with point monitoring ground based gauges. The 2D-Video-Distrometer allows for a detailed verification of rain intensity measurements. Before discussing a comparison of weather radar versus 2D-Video-Distrometer a comparison to a standard tipping bucket raingauge is presented.

3.1 2D-Video-Distrometer versus tipping bucket raingauge

In addition to the calibration of the 2D-Video-Distrometer by use of high-precision spheres, distrometer data have been validated in comparison with a standard raingauge. In widespread rain situations with moderate rainrates tipping bucket raingauges promise to be reliable.

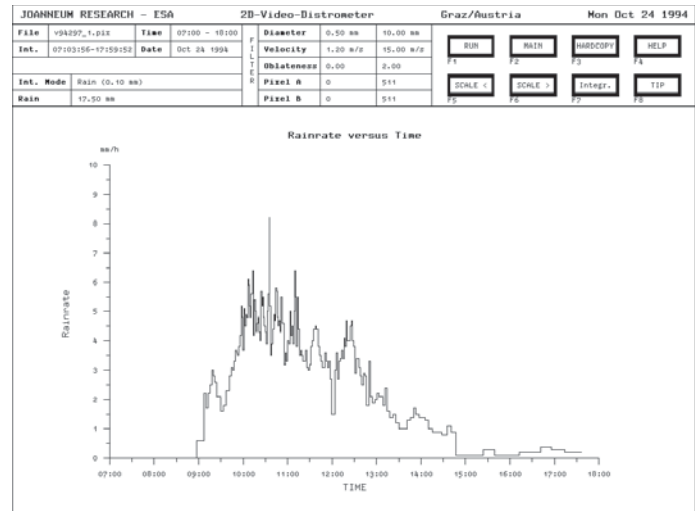


Figure 12: Rainrate vs. time due to distrometer, processed with 0.1 mm integration interval

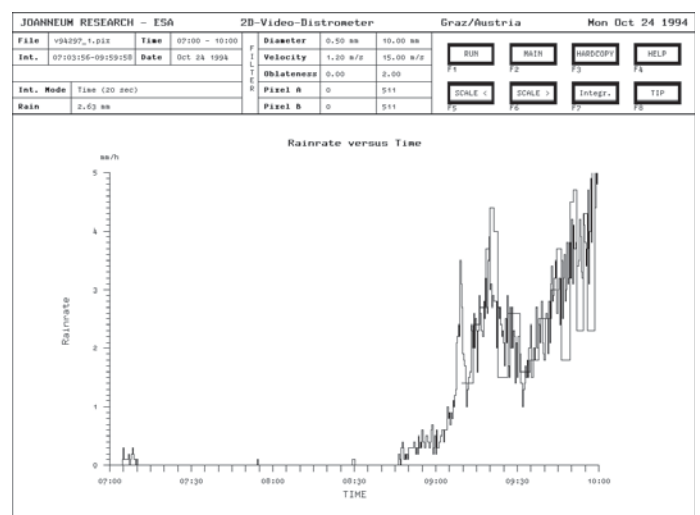


Figure 13: Beginning of event shown in fig. 12, distrometer with 15 sec. integration interval, compared to 0.1 mm tipping bucket raingauge

Figure 12 presents a rainrate versus time diagram. A widespread rain event of October 24, 1994 in Graz/Austria is presented, lasting several hours with rainrates not exceeding 10 mm/hr. The result of the 2D-Video-Distrometer is presented, a short outage of less than 2 minutes due to a system synchronisation process at 12:00 is recognised. The integration criterion for this figure is the same as with a nearby tipping bucket raingauge (0.1 mm rain). The two devices have been installed in a distance of 21 meters. Rain total is given by the distrometer to be 17.5 mm and by the tipping bucket raingauge to be 18.7 mm, the overall comparison is better than 7 percent. Figure 13 presents

the beginning of the rain event. For this figure the integration interval of the distrometer has been set to 15 seconds. There was continuing light drizzle since 07:04, when the distrometer counted the first drops. The raingauge took some time to collect the first bucket of water, it sent the first tipping at 09:10.

3.2 Weather Radar versus 2D-Video-Distrometer

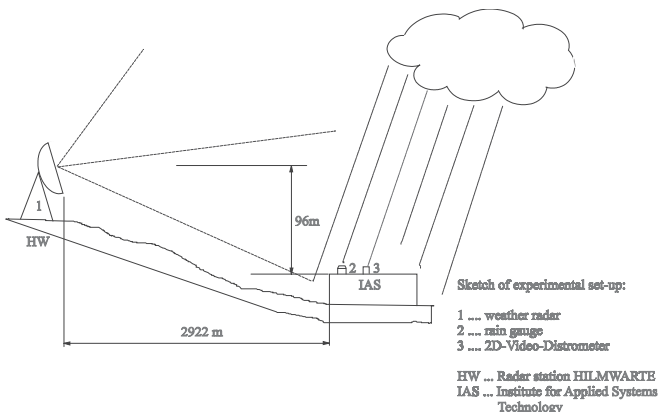


Figure 14: Experimental setup for comparison of radar and distrometer data

Weather radar data have been compared with 2D-Video-Distrometer data. The experimental setup shall shortly be explained by the sketch given in figure 14. The weather radar station Graz/Hilmwarte (HW) is equipped with a C-band dual-polarisation frequency agile weather radar. In 2922 m distance, at the location of the Institute for Applied Systems Technology (IAS), the tipping bucket raingauge and the 2D-Video-Distrometer are installed. Height distance from HW down to IAS is 96 meters. Radar data applied in the following analysis have been extracted from RHI scans over IAS. In order to avoid clutter influence even in the sidelobes, only data at 5 degrees elevation angle have been used, resulting in a height of 352 m between the considered radar echo cell and the ground monitoring instruments at IAS.

A storm recorded on May 7, 1993 is discussed. Between 13:20 and 13:35 a storm happened with rainrates measured at the ground of up to 62 mm/hr. An early prototype of the 2D-Video-Distrometer has been used. The conversion of radar measured copolar horizontal reflectivity ZH to rainrate via standard model assuming drops size distribution (DSD) by Marshall and Palmer (1948) indicates more than 106 mm/hr. Figure 15 presents a rainrate versus time diagram. The solid line indicates rainrate measurements by the distrometer, the markers stand for the radar derivations using ZH and Marshall and Palmer (1948) DSD. Obviously the radar interpretation strongly overestimates the rainrate measured at the ground. Switching over to the ZH versus time diagram (figure 16) the radar measured ZH

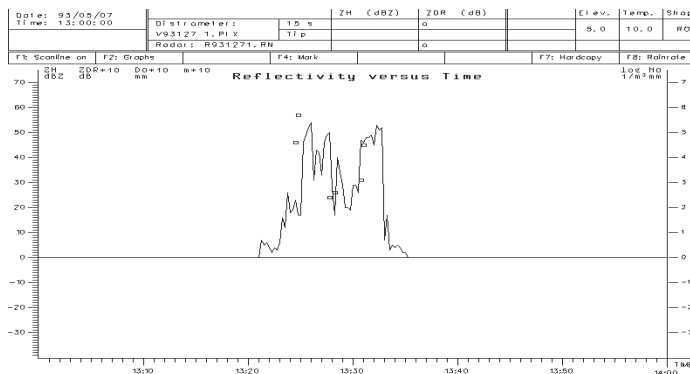


Figure 15: Rainrate vs. time of storm May 7, 1993 (13:00 - 14:00)

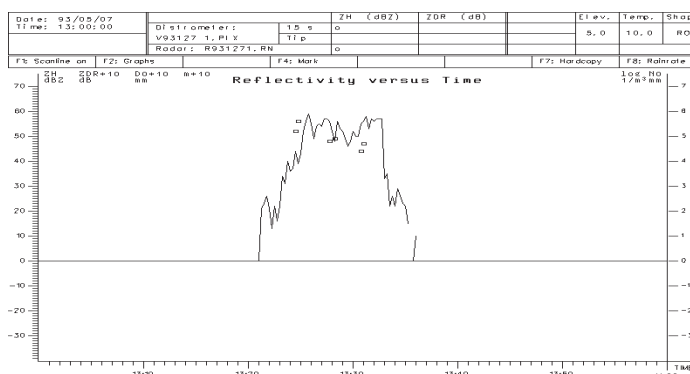


Figure 16: ZH vs. time (same period as fig. 15)

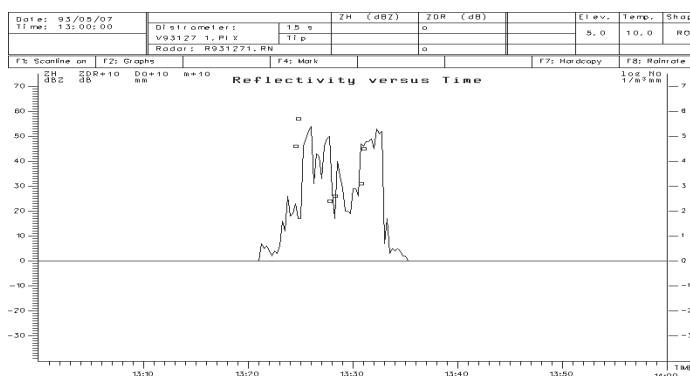


Figure 17: ZDR vs. time (same period as fig. 15 and fig. 16)

and distrometer derivation match fairly well. Radar maximum ZH is 56.36 dBZ, one minute later the distrometer proposes 59.15 dBZ, even exceeding radar measurements. It has to be taken into account that fall time and wind certainly impair the match in the comparison. The differential reflectivity ZDR has been compared as well (figure 17). Distrometer derived ZDR has been calculated by means of measured DSD and a standard model for drop oblateness (Poiars Baptista, 1992). Due to lack of a suitable program the distrometer measured shapes have not been the basis for calculation of precipitation particle scattering amplitudes. Whereas the comparisons of ZH and ZDR yield a fairly good match the results in the rainrate are contradictory. The reason has to be one of the assumptions made in the conversion from radar reflectivities to rainrates. The conversion from reflectivities to rainrates uses models for the DSD, whereas in the other

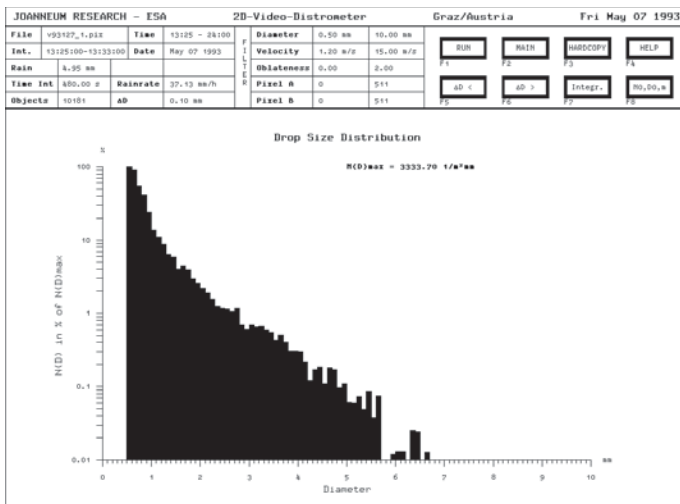


Figure 18: DSD measured by distrometer (13:25-13:33)

way round, from distrometer measurements to reflectivities the measured DSD is used. The difference of actual measured DSD to standard models is significant, it may result in considerable misinterpretation of weather radar data in terms of rainfall. Figure 18 presents the DSD resulting from the distrometer measurements between 13:25 and 13:33 representing 4.95 mm of rainfall at a mean rainrate of 37.1 mm/hr. These eight minutes represent the main part of the event, 97 percent of the total rain in this event has fallen in that period. Converting this DSD to reflectivities by means of conversion of the individual size classes yields expected radar reflectivities of 55.08 dBZ in ZH and 4.36 dB in ZDR. On the other hand recalculating the rainrate from 55.08 dBZ by means of inverting the relation $Z=200 \cdot R^{1.6}$ yields more than 100 mm/hr rainrate in clear contradiction to the measured 37.1 mm/hr. An improvement may be achieved by the use of ZH and ZDR to determine the parameters of a two-parametric exponential DSD. Inverting 55.08 dBZ of ZH and 4.36 dB of ZDR yields a rainrate of 58 mm/hr for that timeperiod of 8 minutes, which is clearly a better result than the one-parametric approach using ZH only.

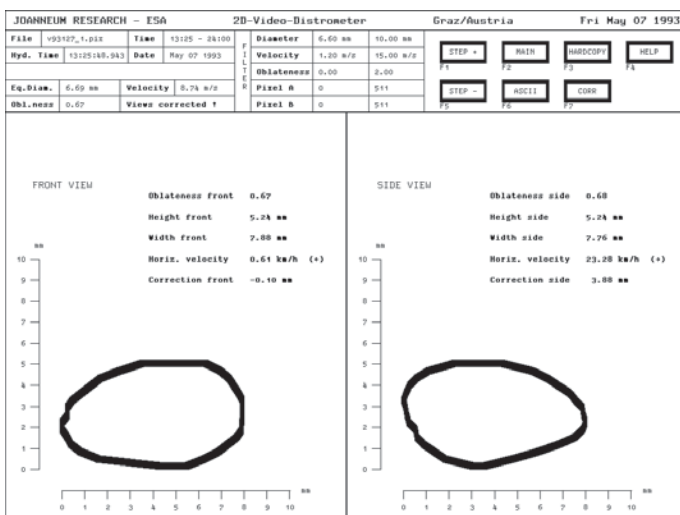


Figure 19: Drop views at high end of DSD

As an example in figure 19 the front and the side view of one of the big drops are given, they contribute much to the high reflectivity values. Table 1 summarizes the numeric results:

time	distrometer measured rainfall	distrometer derived ZH	distrometer derived ZDR	reconversion of distrometer derived ZH to rainfall	reconversion of distrometer derived ZH and ZDR to rainfall
12:25-12:33	37.1 mm/h	55.08 dBZ	4.36 dB	101 mm/h	58 mm/h

Table 1: Overview on results and derivates based on measured DSD shown in figure 18

4. SUMMARY AND CONCLUSIONS

Measurements have been done using a 2D-Video-Distrometer, a standard tipping bucket rain gauge and a C-band dual-polarisation frequency agile weather radar. The 2D-Video-Distrometer is a newly developed precipitation gauge, it measures rainrate as well as all particularities of single hydrometeors and allows classifications of precipitation events. Raindrops, melting particles and snowflakes have been presented. Effects like drop oscillation and distortions due to horizontal wind have been qualitatively described. In situations with no wind drop shapes do not differ significantly from standard models, only drop's oblatenesses are significantly spread around their mean value. In storm situations quite irregular drop shapes have been recorded. Many drops are flattened at the side, obviously due to horizontal wind forces. Further work should be done to obtain quantitative results on drop oscillations and distortions. Drop's scattering amplitudes should be calculated on the basis of measured shapes. Fall velocities of hydrometeors have been measured as well and have been compared to models taken from the literature. In calm widespread rain events fall velocities follow closely the expected values taken from the literature, in storm events they are widely spread around the expected values. Measurement of fall velocities allows a precise normalisation from the number of drops reaching the measuring area to the volume above. Comparisons of rainrates measured by the distrometer and by the tipping bucket rain gauge reveal a good match. Data recorded during a storm event in Graz/Austria show that conversions of radar reflectivities to rainrates using standard drop size distributions lead to significant misinterpretations whereas comparisons of radar reflectivities and reflectivities derived from distrometer data reveal a good match. The explanation for this discrepancy is, that the conversion of distrometer data to reflectivities is based on the measured drop size distributions whereas the conversion of radar reflectivities to rainfall parameters uses standard models for drop size distributions.

In this paper measurements of precipitation parameters have been presented, indicating noticeable differences to standard models. It has been shown that the use of standard models may lead to significant misinterpretations of weather radar reflectivities. Considering the great importance of weather radar technology and its wide use it is recommended, that further investigations should be done. Based on a statistically reliable data base standard models shall be verified and improved where necessary.

5. REFERENCES

Atlas, D., R. C. Shrivastava and R. S. Sekhon, 1973, "Doppler radar characteristics of precipitation at vertical incidence", Rev. Geophys. Space Phys., Vol. 2

Gunn, R. and G. D. Kinzer, 1949, "The terminal velocity of fall for water droplets in stagnant air", J. Meteorol., Vol. 6, pp. 243 - 248

Marshall, J. S. and W. McK. Palmer, 1948, "The distributions of raindrops with size", J. Meteorol., Vol. 5, pp. 165 - 166

Morrison, J.A. and M.-J. Cross, 1974, "Scattering of a plane electromagnetic wave by axisymmetric raindrops", The Bell System Technical Journal, Vol. 53, pp. 955 - 1019

Poiares Baptista, J. P. V., 1992, "OPEX radar group - call for scattering calculations", Proceedings of the 17th Meeting of Olympus Propagation Experimenters, Stockholm/Helsinki, May 3 - 5th 1992, p. 39

Pruppacher, H.R. and K.V. Beard, 1970, "A wind tunnel investigation of the internal circulation and shape of water drops falling at terminal velocity in air", Quart. J. R. Meteorol. Soc., Vol. 96, pp. 247 - 256

The work described in this paper has been done
under ESA/ESTEC contract no.
9949/92/NL/PB(SC)